1	How frequently does rapid intensification occur after rapid contraction of the					
2	radius of maximum wind in tropical cyclones over the North Atlantic and					
3	Eastern North Pacific?					
4	Yuanlong Li <sup>1</sup> , Yuqing Wang <sup>2*</sup> , Zhe-Min Tan <sup>1</sup>					
5	<sup>1</sup> School of Atmospheric Sciences, Nanjing University, Nanjing, China					
6	<sup>2</sup> International Pacific Research Center and Department of Atmospheric Sciences, School of					
7	Ocean and Earth Science and Technology, University of Hawaii at Manoa, Honolulu, Hawaii,					
8	USA					
9	December 2, 2021 (resubmitted)					
10	January 24, 2022 (first revision)					
11	March 4, 2022 (second revision)					
12	April 3, 2022 (Third revision)					
13	Dateline					
14	Submitted to Monthly Weather Review					
15	*Corresponding author address:					
16	Prof. Yuqing Wang					
17	International Pacific Research Center					
18	University of Hawaii at Manoa					
19	404A/POST, 1680 East West Road,					
20	Honolulu, HI 96822, USA.					
21	Email: yuqing@hawaii.edu					

### 22 ABSTRACT

23

24

25

26

27

28

29

30

31

32

33

34

35

36

37

38

The phenomenon that rapid contraction (RC) of the radius of maximum wind (RMW) could precede rapid intensification (RI) in tropical cyclones (TCs) has been found in several previous studies, but it is still unclear how frequently and to what extent RC precedes RI in rapidly intensifying and contracting TCs in observations. In this study, the statistical relationship between RMW RC and TC RI is examined based on the extended best-track dataset for the North Atlantic and Eastern North Pacific during 1999–2019. Results show that for more than ~65% of available TCs, the time of the peak contraction rate precedes the time of the peak intensification rate, on average, by ~10-15 h. With the quantitatively defined RC and RI, results show that ~50% TCs with RC experience RI, and TCs with larger intensity and smaller RMW and embedded in more favorable environmental conditions tend to experience RI more readily following an RC. Among those TCs with RC and RI, more than ~65% involve the onset of RC preceding the onset of RI, on average, by ~15–25 h. The preceding time tends to be longer with lower TC intensity and larger RMW and shows weak correlations with environmental conditions. The qualitative results are insensitive to the time interval for the calculation of intensification/contraction rates and the definition of RI. The results from this study can improve our understanding of TC structure and intensity changes.

1

### 1. Introduction

One of the most important and difficult challenges in tropical cyclone (TC) forecasting is the prediction of rapid intensification (RI, Kaplan et al. 2015; Knaff et al. 2020), often defined as the intensification rate being at least the 95th percentile of all TC intensity changes over water (e.g., ≥ 30 kt or 15.4 m s<sup>-1</sup> within 24 h in the North Atlantic; Kaplan and DeMaria 2003). RI is difficult to forecast due to the multiscale interactions associated with both internal and environmental dynamical and physical processes, most of which are not fully understood (Wang and Wu 2004; Emanuel 2018).

A key issue in understanding the RI internal dynamics is the relationship between changes in TC intensity and structure. Based on the convective ring model of TC intensification, it has long been known that TC intensification is often related to contraction of the radius of maximum wind (RMW; Shapiro and Willoughby 1982; Schubert and Hack 1982; Willoughby 1990). However, several recent studies have shown that RMW contraction often stops well before the end of intensification partly due to the increased curvature of the radial profile of tangential wind and/or the decreased negative radial gradient of tangential wind tendency at the RMW during the late intensification stage (Stern et al. 2015; Li et al. 2019), and both prohibit further contraction of the RMW. Previous studies have also found that rapid contraction (RC) of RMW could precede TC RI in both observations and simulations (Corbosiero et al. 2005; Chen et al. 2011; Shimada and Horinouchi 2018; Wu and Ruan 2021; Li et al. 2021).

Based on budgets of tangential wind and RMW using ensemble idealized axisymmetric TC simulations, Li et al. (2021) recently showed that in the initial intensification stage, the moderate low-level negative radial gradient of tangential wind tendency and small curvature of the radial profile of tangential wind favor RC, but the weak inner-core diabatic heating far inside the RMW and relatively weak absolute vorticity lead to a weak intensification rate. As the simulated TC continues to contract its RMW and intensify, the greater inner-core diabatic heating closer to the RMW, where absolute vorticity also becomes larger, supports a much larger low-level radial vorticity flux, which allows for more RI, but the increasing curvature of the wind profile prevents further RC. The results of Li et al. (2021) seem to suggest that RMW RC tends to precede TC RI, because in the early intensification stage, the curvature of the radial profile of tangential wind, which limits the RMW contraction, generally increases as a TC intensifies (Stern et al. 2015; Li et al. 2019). The low-level TC intensification is dominated by the radial vorticity flux, which

generally increases as a TC intensifies due to the increase in both the absolute vertical vorticity and the radial inflow near the RMW associated with the increasing diabatic heating in the eyewall (Li et al. 2019, 2021).

Results from statistical analyses by Xu and Wang (2015) and Wu and Ruan (2021) also showed that RI often occurs after the RMW contracts to a certain small size. However, there is no observational study to confirm how frequently and to what extent the RMW RC precedes TC RI in rapidly intensifying and contracting TCs, and how frequently and under what conditions TCs tend to experience RI following an RC. Although the statistical study of Wu and Ruan (2021) showed that in the North Atlantic during 2000–2017 the number of TCs with RMW RC preceding RI is comparable to the number of TCs with RMW RC occurring simultaneously with RI, the events of RC preceding RI in their study were incomplete because those events with overlapping 24-h RI and 24-h RC were excluded (Q. Wu, personal communication). Namely, only if the initial time of 24-h RC precedes that of the 24-h RI by more than 24 h, can a TC be regarded as an event of RC preceding RI in their study.

The primary objective of the current study is to investigate whether and to what extent RMW RC tends to precede TC RI, and how frequently TC RI occurs following RMW RC and the potential factors affecting the occurrence of RI following RC in observations. We first compare the times of the lifetime peak rate of contraction and intensification of each TC from observational data, similar to those in Li et al. (2021). Then, the relationship between the onset times of the quantitatively defined RC and RI of each TC is examined. The next section describes the observational dataset, data processing, and analysis method. The comparison between the times of TC lifetime peak contraction rate and peak intensification rate is discussed in section 3. Section 4 statistically compares the onset times of the quantitatively defined RC and RI. Section 5 discusses the potential impacts of TC characteristics and some environmental parameters on the occurrence of RI following an RC. Section 6 discusses the potential impacts of TC intensity and structure as well as some environmental parameters on the preceding time of the onset of RC relative to the onset of RI in rapidly intensifying and contracting TCs. Concluding remarks are drawn in the last section.

# 2. Data and analysis method

As in Qin et al. (2016) and Wu and Ruan (2021), the extended best-track (EBT) dataset (Demuth et al. 2006) at 6-h interval is used in this study. The dataset of version 3.0.0 updated in

March 2021 is used here, which has been extended to use all data available in the National Hurricane Center Best Track Data (HURDAT2, Landsea and Franklin 2013). The dataset contains TCs in the North Atlantic during 1851–2019, the Central North Pacific during 1950–2019, and the Eastern North Pacific during 1949–2019. Note that the RMW information is only available since 1988 for all three basins in the dataset, and the Advanced Microwave Sounding Unit (AMSU) was used to identify and analyze TCs since 1999 (Demuth et al. 2004), in which the horizontal resolution is more than doubled that of its previous Microwave Sounding Unit (MSU). Wu and Ruan (2021) also showed that the RMW data in the EBT dataset were of better quality since 1999 (see their supplementary information). Therefore, to ensure the reliability of the main results, only those TCs during 1999–2019 were considered in this study. There are 356, 33, and 379 TCs in the North Atlantic, Central North Pacific, and Eastern North Pacific, respectively, during this period. Because of the limited sample size, TCs in the Central North Pacific will not be included in our analysis. For each TC at a given time, the record in the dataset contains maximum sustained 10-m wind speed (Vmax), minimum central sea-level pressure (Pmin), RMW, eye size, radius of 17.5 m s<sup>-1</sup> wind in four quadrants, distance to the nearest major landmass, and an indicator of whether the system is purely tropical, subtropical, or extra-tropical.

In all analyses in this study, those TCs with the lifetime maximum *Vmax* weaker than category-1 hurricane (33 m s<sup>-1</sup>) are excluded as in Qin et al. (2016). With this criterion there are 157 and 175 TCs retained in the North Atlantic and Eastern North Pacific, respectively. Following Kimball and Mulekar (2004) and Kossin et al. (2007), a quality check has been performed for the RMW information. Namely, those RMW records with RMW smaller than the radius of eye or greater than the mean radius of 17.5 m s<sup>-1</sup> wind are marked as missing information. As in Wu and Ruan (2021), for each calculation of intensification rate or contraction rate, including the definitions of RI and RC discussed in section 4, those records with distance to the nearest major landmass less than 100 km are excluded to reduce the effect of land interaction on the results. Those records that are identified as subtropical or extra-tropical systems are also excluded.

To compare the times of the peak RMW contraction rate and peak TC intensification rate or the onset times of RC and RI, several additional objective criteria are used to obtain the available TCs for the comparison. First, TCs with missing either RMW or intensity information are discarded, and only those TC records before the TC attains the lifetime maximum intensity are included in the analysis to ensure to cover the intensification period only. This means that the reintensification

of TCs after the eyewall replacement cycle or TCs that weakened crossing the Florida Peninsula, Cuba, or Yucatan Peninsula and subsequently reintensified (e.g., Willoughby et al. 1982; Kossin and Sitkowski 2009; Mauk 2016; Mainelli et al. 2008) was largely excluded in our analysis. Second, considering the fact that the estimation error of TC wind profile from available data is larger for weaker storms (Kossin et al. 2007), to make the comparison as robust as possible, we only include all TCs in the records with the intensity attaining tropical storm (≥18 m s<sup>-1</sup>). Third, only those TCs with the period of intensification (contraction) being greater than four consecutive times (i.e., 24 h) are considered to reduce the effect of short record on the comparison between the times of the peak contraction rate and peak intensification rate or the onset times of RC and RI. Finally, in addition to *Vmax*, *Pmin* is also used for the calculation of intensification rate in the comparison between the onset times of RC and RI to ensure the robustness of the results.

Furthermore, considering the fact that the statistical results of intensification rate and contraction rate may depend on the time interval (Qin et al. 2016), in addition to the commonly used 24-h interval as in previous studies, the results based on 18-h, 12-h, and 6-h intervals are also evaluated to ensure the robustness of the main results from this study. The criteria for 18-h, 12-h, and 6-h intervals are the same as those for the 24-h interval. The corresponding intensification (contraction) rate for each time interval at each time,  $t_0$ , is defined as the average change (decrease) rate of intensity (RMW) from  $t_0$  to  $t_0$ + interval.

# 3. Times of the peak contraction rate and peak intensification rate

Based on those criteria in section 2, in the dataset there are 205, 235, 263, and 284 TCs available during 1999–2019 in the North Atlantic and Eastern North Pacific for the comparison between the times of the peak RMW contraction rate and the peak TC intensification rate at the time intervals of 24 h, 18 h, 12 h, and 6 h, respectively. Note that because it is easier to have a longer consecutive period of intensification (contraction) using a shorter time interval (for example, for a 30-h record, the consecutive times are 5 and 2 for the 6-h and 24-h time intervals, respectively), the available TC count increases with the decrease in time interval. Of those available TCs, ~65–75%, ~15–20%, and ~15–20% involve the time of the peak contraction rate preceding, occurring simultaneously with, and lagging the time of the peak intensification rate, respectively (Fig. 1e). Since the estimation error of TC wind profiles from available data is generally smaller for stronger storms (Kossin et al. 2007), for those TCs that have multiple times of peak intensification rate or

peak RMW contraction rate, the last time of those peak RMW contraction records is defined as the time of peak contraction rate, and the nearest peak intensification record to the defined time of peak contraction rate is defined as the time of peak intensification rate in our analysis. We have also compared the results with those using the first time or the average time of those peak RMW contraction records and found that the qualitative results are almost unchanged, i.e., more than ~65% TCs involve the time of the peak contraction rate preceding the time of the peak intensification rate (not shown). The result is also almost independent of the time interval used for the calculations of contraction rate and intensification rate (Fig. 1e). As expected, consistent with that implied by the results in Li et al. (2021), the time of the peak contraction rate predominantly precedes the time of the peak intensification rate. In addition, the result is independent of the basin as well (Figs. 1a,c,e).

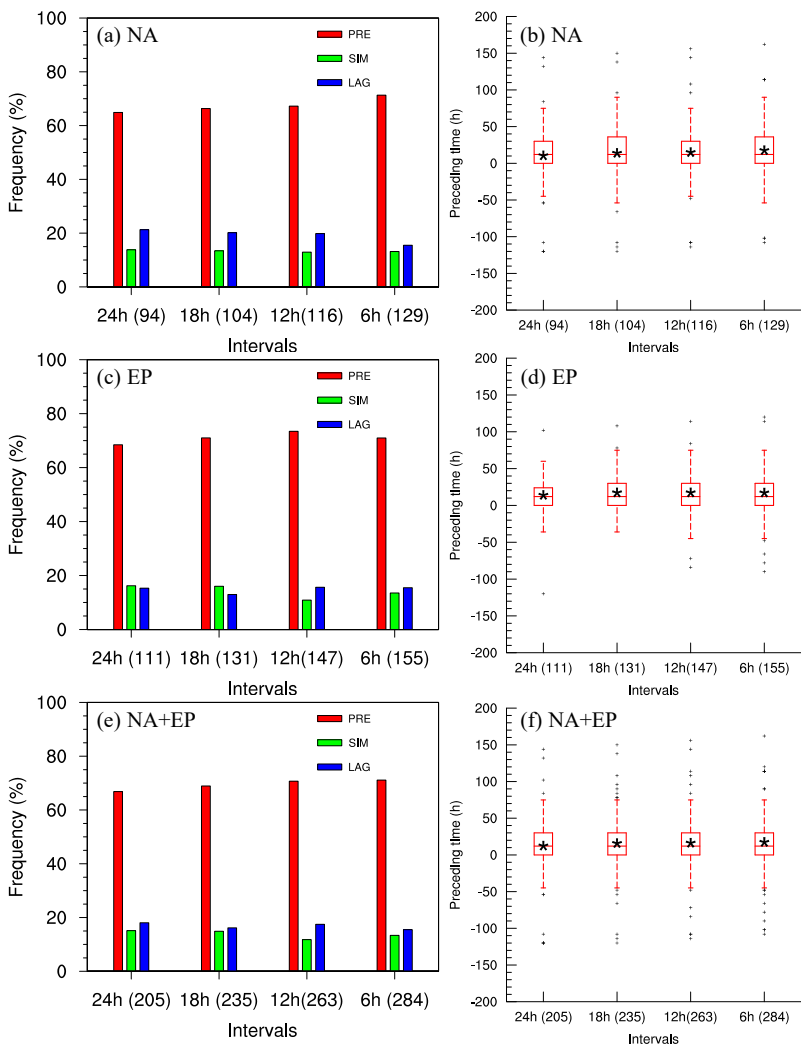


Figure 1. (a) Frequency of TCs with the time of the peak RMW contraction rate preceding (PRE), occurring simultaneously (SIM) with, and lagging (LAG) the time of the peak intensification rate in the North Atlantic (NA) with the intensification and contraction rates calculated with the time intervals of 24 h, 18 h, 12 h, and 6 h, respectively, with the total available number of TCs for each time interval shown in the parentheses following

each *x*-axis label. (b) Boxplots of difference between the times of the peak intensification rate and peak RMW contraction rate in the North Atlantic (NA) based on the time intervals of 24 h, 18 h, 12 h, and 6 h, respectively. The bottom and top edges of each box denote the 25th and 75th percentiles, and the horizontal line inside the box is the median. The black asterisk denotes the average. The bottom and top whiskers extend to the minimum and maximum within a distance of 1.5 times of the interquartile, and the outliers (outside the whiskers) are plotted with the black plus sign. (c)–(d) As in (a)–(b), but for the results in the Eastern North Pacific (EP). (e)–(f) As in (a)–(b), but for the results in both the North Atlantic and the Eastern North Pacific (NA+EP).

To further quantify the difference between the times of the peak TC intensification rate and peak RMW contraction rate, we show the corresponding boxplot in Figs. 1b,d,f based on those selected TCs. Consistent with Figs. 1a,c,e, for each basin and for each time interval, more than ~70% of the differences are greater than zero, indicating that the time of the peak contraction rate predominantly precedes the time of the peak intensification rate. From Figs. 1b,d,f, we can also see that more than 50% of the differences are between ~0-30 h, and on average (including the simultaneous cases and lag cases), the time of the peak contraction rate precedes that of the peak intensification rate by  $\sim 10-15$  h. Overall, the results for the two basins are qualitatively consistent, although there are more outliers in the North Atlantic than in the Eastern North Pacific (Figs. 1b,d). Since the aircraft reconnaissance is rarely conducted in the Eastern North Pacific, the consistent results between the North Atlantic and Eastern North Pacific (Figs. 1a-d) indicate that the dataset may not be affected by the non-aircraft data, as also suggested by Kimball and Mulekar (2004). In addition, the results with the intensification and contraction rates calculated using different time intervals are also qualitatively consistent, although the number of outliers increases with the decreasing time interval, especially in the Eastern North Pacific (Figs. 1b,d). This is because it is easier to obtain an extreme intensification (contraction) rate for a shorter time interval. The outliers are also quantitatively affected by the definition of the time of peak intensification rate or peak contraction rate in those TCs that have multiple times of peak intensification rate or peak RMW contraction rate (not shown). Since the outliers are not our focus and most of them occur with the peak contraction and peak intensification being in the different dynamical process (not shown), we do not go into details on the outliers.

#### 4. The onset times of RC and RI

176

177

178

179

180

181

182

183

184

185

186

187

188

189

190

191

192

193

194

195

196

197

198

199

200

201

202

203

204

205

206

207

208

Results discussed in the last section confirm that the peak contraction rate tends to precede the peak intensification rate in observations. A further issue is the relationship between the onset times of the quantitatively defined RC and RI. Following Kaplan and DeMaria (2003), the RC and RI are defined as the 95th percentile of all RMW contracts and TC intensity changes over water,

respectively, with the data based on those criteria outlined in section 2 (second paragraph). Figure 2 shows the cumulative frequency distributions of intensification rates for different TC intensities (i.e., tropical depressions with  $Vmax < 18 \text{ m s}^{-1}$ , tropical storms with  $18 \text{ m s}^{-1} \le Vmax < 32 \text{ m s}^{-1}$ , and hurricanes with  $Vmax \ge 32 \text{ m s}^{-1}$ ) and RMWs (i.e., small size with RMW < 30 km, moderate size with  $30 \text{ km} \le \text{RMW} < 60 \text{ km}$ , and large size with RMW  $\ge 60 \text{ km}$ ) in the North Atlantic and Eastern North Pacific during 1999–2019. Note that the cumulative frequency distributions of intensification rates and contraction rates discussed below are qualitatively consistent in the North Atlantic and Eastern North Pacific, and we thus only show their combined distributions.

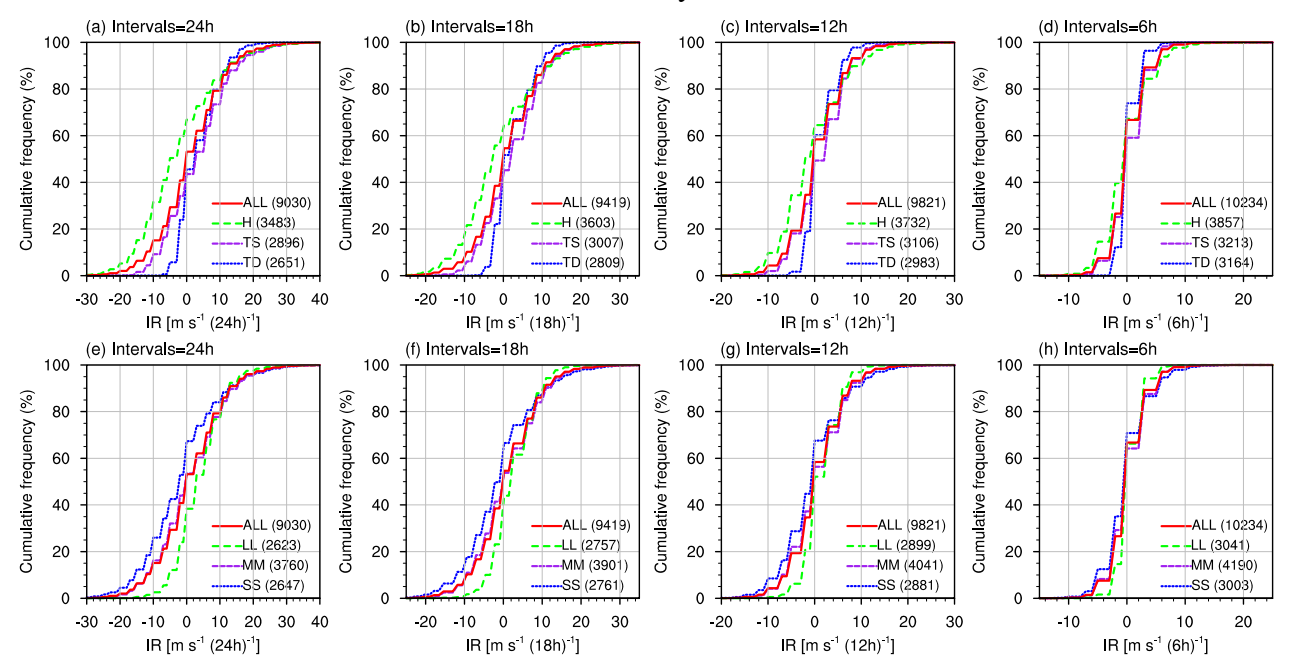


Figure 2. Cumulative frequency distributions of intensification rate (IR) in the North Atlantic and Eastern North Pacific during 1999–2019 based on the (a,e) 24-h, (b,f) 18-h, (c,g) 12-h, and (d,h) 6-h time intervals. Distributions in (a)–(d) are for tropical depressions (TD;  $Vmax < 18 \text{ m s}^{-1}$ ), tropical storms (TS;  $18 \text{ m s}^{-1} \le Vmax < 32 \text{ m s}^{-1}$ ), hurricanes (H;  $32 \text{ m s}^{-1} \le Vmax$ ), and all TCs (ALL), with the corresponding sample number of intensification rate shown in the parentheses of each legend. (e)–(h) As in (a)–(d), but for small (SS; RMW < 30 km), moderate (MM;  $30 \text{ km} \le RMW < 60 \text{ km}$ ), large (LL;  $60 \text{ km} \le RMW$ ) RMW, and all TCs (ALL).

The percentage of the positive intensification rate decreases with increasing TC intensity, and vice versa (Figs. 2a–d), consistent with Kaplan and DeMaria (2003), indicating that TCs with weaker intensity are easier to intensify. This is partly because TCs with weaker intensity usually have more potential to intensify than those with stronger intensity as shown in Xu and Wang (2015). In addition, TCs with large RMWs show less frequent large weakening or intensification rates (Figs. 2e–h). This is understandable because RI often occurs after the RMW contracts to a relatively small size as recently shown in Wu and Ruan (2021), and large RMWs usually occur during the weak-

intensity period (e.g., Wu and Ruan 2021; Li et al. 2021), which has less potential to experience rapid intensification or weakening (Xu and Wang 2015; Fei et al. 2020). Note that although the cumulative frequency distributions in the two basins are qualitatively consistent (not shown), there are some quantitative differences. Overall, for all TCs, the RI thresholds for all time intervals are larger in the Eastern North Pacific than in the North Atlantic (Table 1). For example, the 95th percentile of intensification rates, i.e., the RI threshold, for the 24-h interval is 15.5 m s<sup>-1</sup> (24 h)<sup>-1</sup> in the North Atlantic (Table 1), consistent with TCs in the North Atlantic during 1989–2000 [Kaplan and DeMaria 2003; 16.0 m s<sup>-1</sup> (24 h)<sup>-1</sup>], but it is 17.9 m s<sup>-1</sup> (24 h)<sup>-1</sup> in the Eastern North Pacific (Table 1). This means that overall the TC intensification rates are higher in the Eastern North Pacific than in the North Atlantic, which has been also reported by Kaplan et al. (2010). Note that Kaplan and DeMaria (2003) used all TCs over water in the North Atlantic but we used hurricanes only as in Qin et al. (2016), and our preliminary tests indicate that the overall conclusions discussed here are not affected with or without considering the hurricane criterion (not shown). Consistent with that in Qin et al. (2016), the RI threshold increases with the decreasing time interval in both basins (Table 1). For example, the RI threshold for the 12-h interval is 10.15 m s<sup>-1</sup> (12 h)<sup>-1</sup> in the North Atlantic, also similar to or 10.0 m s<sup>-1</sup> (12 h)<sup>-1</sup> for the North Atlantic during 1990-2014 (Qin et al. 2016).

231

232

233

234

235

236

237

238

239

240

241

242

243

244

245

246

247

248

249

250

251

252

253

254

255

Table 1. Definitions of RI and RC calculated with the time intervals of 24 h, 18 h, 12 h, and 6 h, respectively, in the North Atlantic (NA) and Eastern North Pacific (EP) during 1999–2019. Note that the unit of rate values are unified into the equivalent change in 24 h for direct comparisons.

Definition	Basin	Intervals=24 h	Intervals=18 h	Intervals=12 h	Intervals=6h
RI [dVmax; m s <sup>-1</sup>	NA	15.5	17.1	20.3	21.4
$(24 \text{ h})^{-1}$ ]	EP	17.9	20.2	20.6	21.5
RI [-dPmin; hPa (24	NA	23.1	24.6	26.3	28.5
h) <sup>-1</sup> ]	EP	25.2	26.7	27.6	28.0
RC [-dRMW; km	NA	55.9	73.6	75.5	75.8
$(24 \text{ h})^{-1}$ ]	EP	46.7	50.4	74.1	74.7

The *Pmin*-based RI is also used to confirm the robustness of the main conclusions based on *Vmax*. The corresponding cumulative frequency distributions of intensification rates for different TC intensities and RMWs are shown in Fig. 3, in which the tropical depressions, tropical storms, and hurricanes are defined as  $Pmin \ge 1000 \text{ hPa}$ , 990 hPa  $\le Pmin < 1000 \text{ hPa}$ , and Pmin < 990 hPa, respectively, following Kantha (2006) and Klotzbach et al. (2020). Similar to the *Vmax*-based

intensification rate, the intensification occurs more readily for weaker TCs (Figs. 3a–d), and TCs with large RMW rarely experience large intensification or large weakening rates (Figs. 3e–h). In addition, the threshold of the *Pmin*-based RI for all TCs also increases with the decreasing time interval in both basins (Table 1), and overall, the RI thresholds are larger in the Eastern North Pacific than in the North Atlantic except for the 6-h time interval.

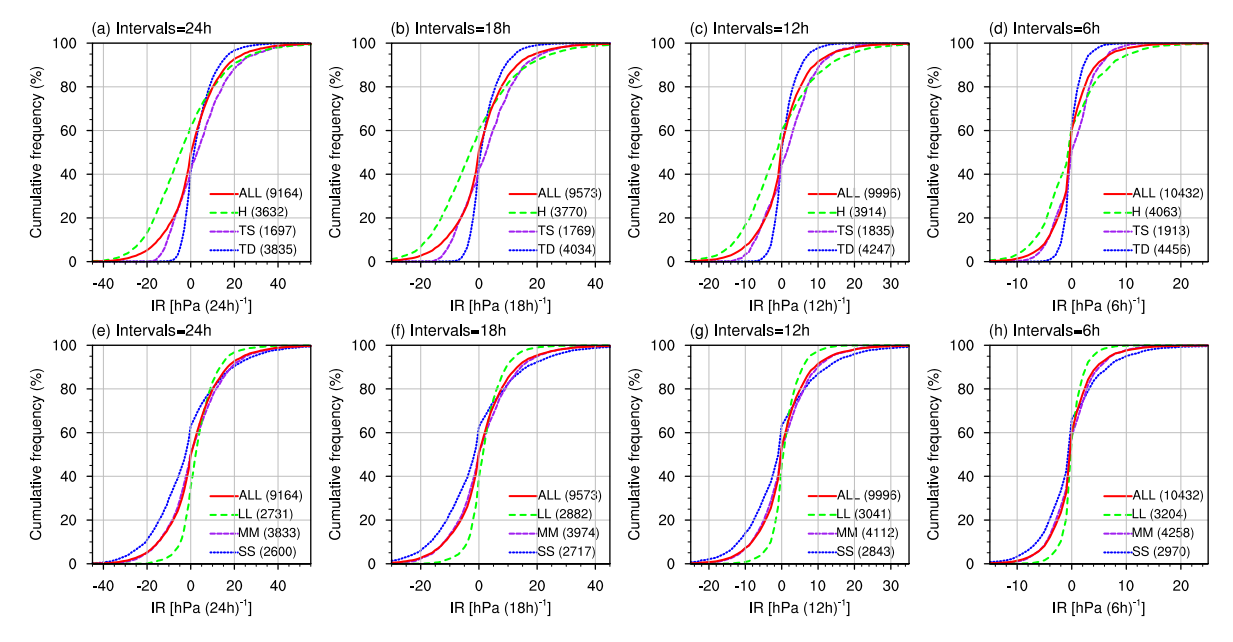


Figure 3. As in Fig. 2, but for the intensification rate (IR) calculated as the deepening rate of minimum central pressure, and tropical depressions (TD), tropical storms (TS), and hurricanes (H) are defined as 1000 hPa  $\leq Pmin$ , 990 hPa  $\leq Pmin$  < 1000 hPa, and Pmin < 990 hPa, respectively.

The cumulative frequency distributions of contraction rates with different TC intensities and RMW sizes are shown in Fig. 4. TCs with weaker intensity (Figs. 4a–d) or larger RMW size (Figs. 4e–h) exhibit more frequent large contraction rates, consistent with previous observational and numerical studies (e.g., Wu and Ruan 2021; Li et al. 2021). This is partly because larger RMW size often means a higher potential to experience large contraction and also often occurs during the weak-intensity stage (Li et al. 2021). In addition, the weaker intensity and larger RMW size often indicate a weaker curvature of the radial profile of tangential wind, thus favorable for large contraction rate (Stern et al. 2015; Li et al. 2021). As expected, the RC threshold for all TCs also increases with the decreasing time interval in both basins (Table 1) as the RI threshold. Overall, the RC threshold is higher for all time intervals in the North Atlantic than in the Eastern North Pacific (Table 1). The RC threshold for the 24-h interval in the North Atlantic is 55.9 km (24 h) <sup>-1</sup>, consistent with that in Wu and Ruan (2021).

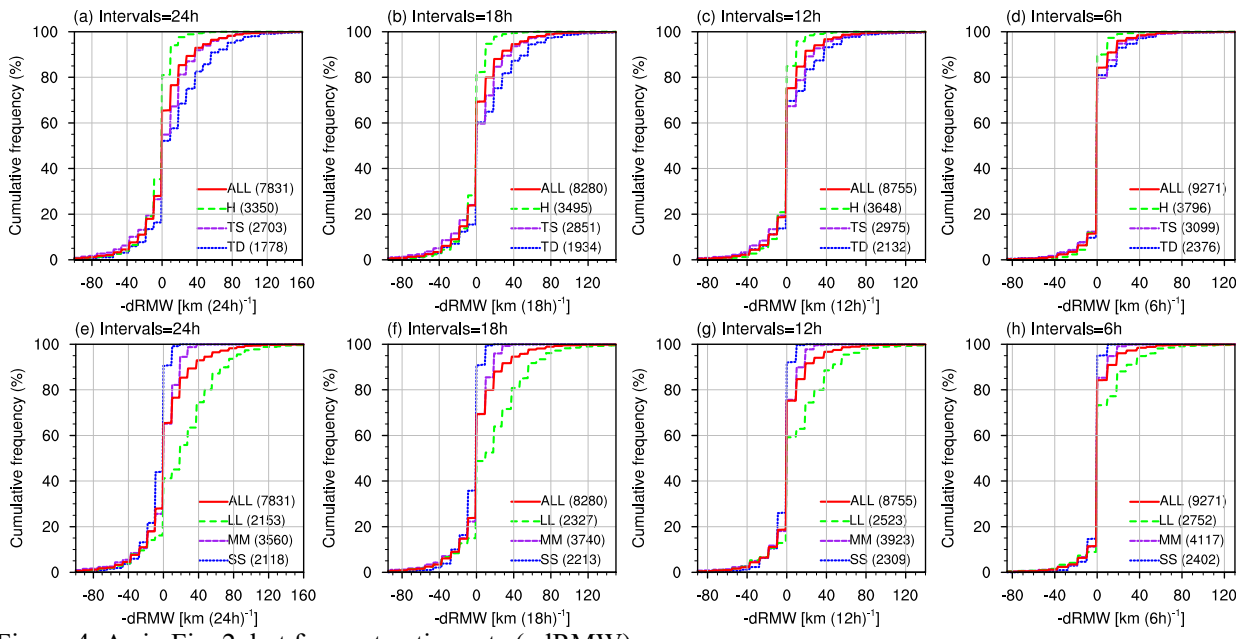


Figure 4. As in Fig. 2, but for contraction rate (-dRMW).

277 278

279

280

281

282

283

284

285

286

287

288

289

290

291

292

293

294

295

296

We now examine the relationship between the onset times of RC and RI based on those TCs satisfied with those criteria described in section 2 (second and third paragraphs) and with the peak intensification rate and the peak contraction rate meeting the corresponding RI and RC thresholds (Table 1). The onset time of RI (RC), for each basin and each time interval, is defined as the first time when the intensification (contraction) rate attains or exceeds the corresponding RI (RC) threshold. The onset times of RC and RI in the North Atlantic and Eastern North Pacific are compared in Figs. 5a,c for each time interval according to the Vmax-based and Pmin-based intensification rates, respectively. Note that the results are qualitatively consistent between in the North Atlantic and Eastern North Pacific (not shown). As expected, for both RI definitions, TCs with the onset of RC preceding the onset of RI are dominant regardless the time interval used. Overall, the percentages of TCs with the onset of RC preceding, occurring simultaneously with, and lagging the onset of RI are  $\sim 65-90\%$ ,  $\sim 5-25\%$ , and  $\sim 0-10\%$ , respectively, for both the *Vmax*based and Pmin-based intensification rates (Figs. 5a,c). Figures 5b,d show the boxplots of the difference between the onset times of RI and RC for the Vmax-based and Pmin-based intensification rates, respectively. In general, for all time intervals, more than ~50% of the differences are between  $\sim 0-36$  h, and on average (including the simultaneous cases and lag cases), the onset of RC precedes the onset of RI by ~15–25 h for both the *Vmax*-based and *Pmin*-based intensification rates.

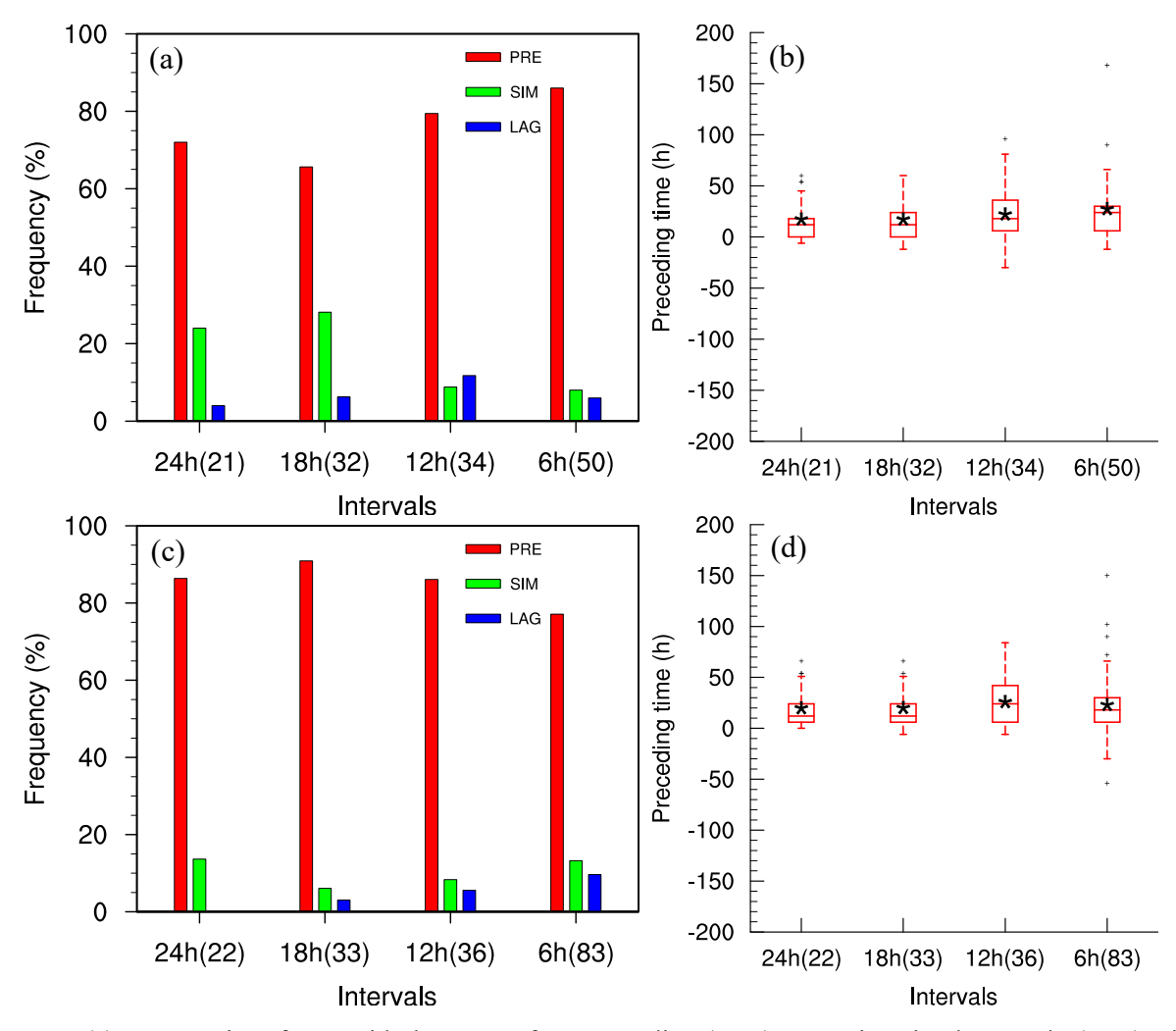


Figure 5. (a) Frequencies of TCs with the onset of RC preceding (PRE), occurring simultaneously (SIM) with, and lagging (LAG) the onset of RI in the North Atlantic and Eastern North Pacific for time intervals of 24 h, 18 h, 12 h, and 6 h, with the total available number of TCs for each interval shown in the parentheses following each *x*-axis label. (b) Boxplots of difference between the onset times of RI and RC. (c)–(d) As in (a)–(b), but for the RI defined using the deepening rate of minimum central sea level pressure.

Note that as mentioned earlier, partly to reduce the effect of eyewall replacement cycle on our results, only those TC records before the TC attains the lifetime maximum intensity are included in the analysis. Considering the fact that only about one-third and 20% TCs with intensity attaining hurricane experience eyewall replacement cycle in the North Atlantic and Eastern North Pacific, respectively (Kossin and Sitkowski 2009; Mauk 2016), and among them ~55% and ~80% occur after/around the TC lifetime maximum intensity (Mauk 2016), we believe that our main conclusions are not affected by the eyewall replacement cycle. To further verify this, we have checked the 21 cases associated with both RC and RI for the 24-h time interval for the *Vmax*-based intensification rate, and there is only one case likely involving the eyewall replacement cycle by looking into the available satellite images (http://tropic.ssec.wisc.edu/real-time/mimtc/tc.shtml),

which occurred after the defined onset times of RC and RI and thus does not affect our results. In addition, we found three cases (including the eyewall replacement cycle case) that involved large RMW expansion (>30 km in 6 h) before the defined onset time of RC, which might be affected by changes in environmental conditions. Since our main conclusions are unchanged with and without the three cases, and considering the fact that the large RMW expansion, especially during the weak TC stage, might be associated with the potential errors in RMW estimation (Demuth et al. 2004, 2006; Kossin et al. 2007), we have not gone into details on the large RMW expansion, which could be a topic for a future work when more reliable data are available.

#### 5. Occurrences of RI and RC

The results discussed in section 4 confirm that, as implied in Li et al. (2021), the onset of RC tends to precede the onset of RI in rapidly intensifying and contracting TCs in observations. However, unlike in the idealized simulations in previous studies (Stern et al. 2015; Li et al. 2021), TCs in observations rarely experience simultaneous RC and RI (cf. Figs. 1,5), partly due to various complicated multiscale interactions associated with both internal and environmental dynamical and physical processes (Wang and Wu 2004). Although we mainly focused on the rapidly intensifying and contracting TCs, from an operational perspective, it would be also relevant to know how frequently RC occurs without RI, and vice versa.

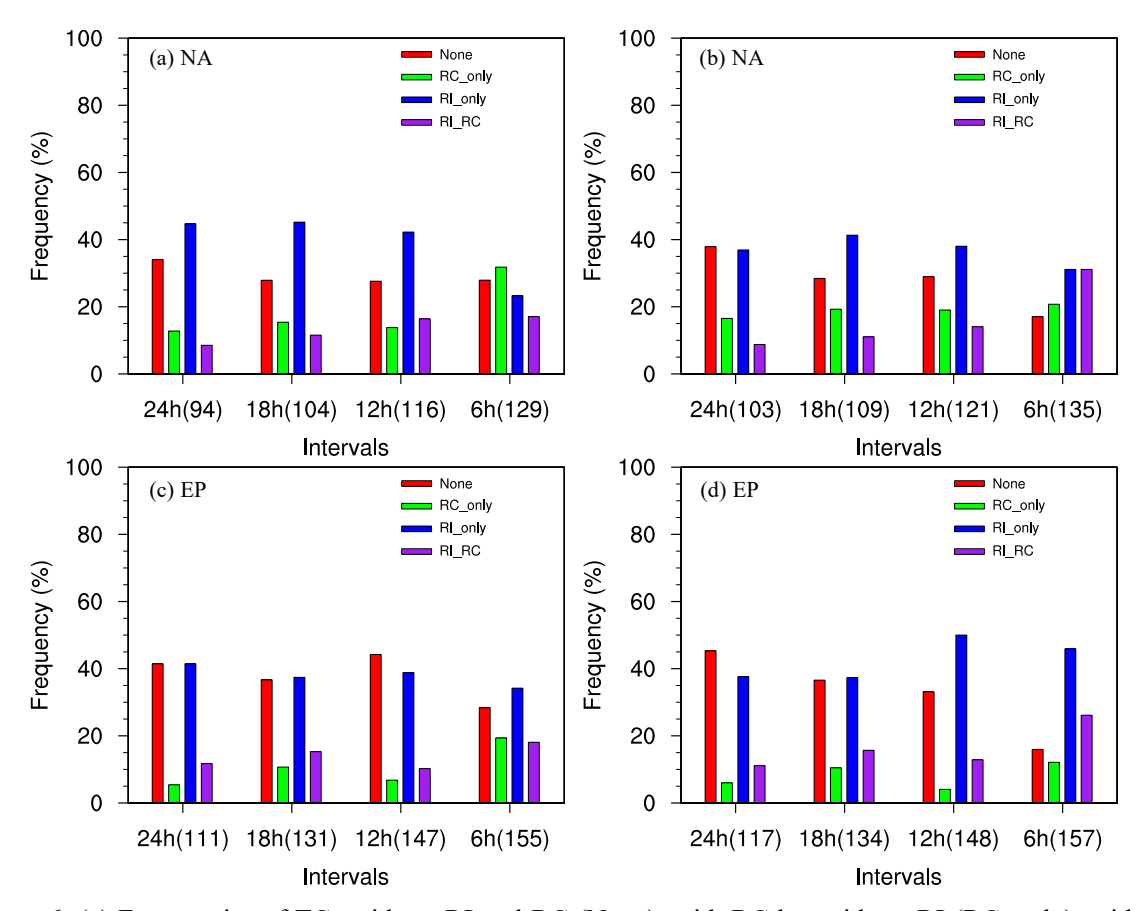


Figure 6. (a) Frequencies of TCs without RI and RC (None), with RC but without RI (RC\_only), with RI but without RC (RI\_only), and with both RI and RC (RI\_RC) in the North Atlantic with the rates calculated using time intervals of 24 h, 18 h, 12 h, and 6 h, with the total available number of TCs for each interval shown in the parentheses following each x-axis label. (b) As in (a), but the RI is defined based on the deepening rate of central sea level pressure. (c)–(d) As in (a)–(b), but for the Eastern North Pacific.

Figure 6 shows the frequencies of TCs without RI and RC, with RC but without RI, with RI but without RC, and with both RI and RC among those available TCs in Fig. 1. The overall frequency distributions are consistent in both basins and for both the *Vmax*-based and *Pmin*-based intensification rates. For both basins, there are ~20–40% TCs that experienced neither RC nor RI, and the frequency decreases with the decreasing time interval, especially for the *Pmin*-based intensification rates (Figs. 6b, d). This is because it is easier to obtain an extreme intensification (contraction) rate for a shorter time interval as mentioned above. In addition, the no RI cases are more prevalent for the *Vmax*-based intensification rates, but less prevalent for the *Pmin*-based intensification rates (Figs. 6a–d). On average, there are up to ~40% of those available TCs that experienced RI but without RC. In addition, for the 6-h time interval, in terms of the *Pmin*-based intensification rates the frequencies of RI with and without RC are nearly equal in the North Atlantic, while the frequency of RI without RC is almost 50% higher in the Eastern North Pacific

(Figs. 6b,d). This suggests that it is not necessary for a TC with RI to experience RC. Previous studies have confirmed that TCs more readily intensify rapidly after the RMW contracts to a certain small size (Xu and Wang 2015; Li et al. 2019; Wu and Ruan 2021). Our results thus suggest that the process of contraction to a certain small size is not necessarily rapid. However, there are some other reasons for the high frequency of TCs with RI but without RC. First, as mentioned in section 2, we have excluded those records with the TC intensity below the tropical storm threshold to make the comparison as robust as possible (Figs. 1, 5), but it cannot rule out the possibility that RC occurs before the tropical storm stage. To verify this, we removed this criterion and found that the averaged frequency of TCs with RI but without RC decrease from ~40% to ~25% as expected (not shown). It is also possible that TCs completed their RCs before being recorded in the EBT dataset. In addition, the RC process in the initial stage of TCs might occur but was missed by the available observations because of the large errors in measuring RMW for weak TCs (cf. Kossin et al. 2007). Considering these uncertainties, the reason for the "missed" RC in the TCs with RI will not be discussed in detail, but it could be a topic for a future work when more reliable data are available.

For TCs with RC, about half experienced RI in the two basins, and the overall ratio of TCs with RI to that without RI is higher in the Eastern North Pacific than in the North Atlantic for both the *Vmax*-based and *Pmin*-based intensification rates (Fig. 6). This means that although RC tends to precede RI in rapidly intensifying and contracting TCs, it does not mean that there must be an RI following an RC. From a practical perspective, it is our interest to further examine the difference between TCs with and without RI following an RC. Since the occurrence of RI involves many known and unknown internal and environmental dynamical and physical processes (Wang and Wu 2004; Emanuel 2018), as a preliminary effort, we only check some commonly known internal and environmental factors. Figures 7a,b show the differences in TC intensity and RMW size immediately following the onset of RC ( $t_0$ + interval with  $t_0$  denoting the onset time of RC) between TCs with RC preceding RI and TCs with RC but without RI in the two basins for each time interval. We can see that on average, TCs with RI following RC have higher intensity and smaller RMW than those without RI, and the results are all statistically significant at the 95% confidence level and consistent for all different time intervals examined and also for the Pminbased intensification rates (Figs. 7e,f). This is consistent with the theoretical study of Li et al. (2021), who has revealed that in the intensification stage, the TC intensification rate is dominated by the low-level radial absolute vorticity flux, which is proportional to the inner-core absolute vorticity, which in turn is a function of TC intensity and its RMW.

In addition, previous observational (Xu and Wang 2015) and recent theoretical studies (Wang et al. 2021a,b) have shown that TC intensification rate often increases with TC intensity and reaches its maximum as the TC reaches an intermediate intensity around 60% of its theoretical maximum potential intensity. Since RC often occurs before the intermediate intensity, this means that, in the early stage following RC, the intensification rate of a TC tends to increase more rapidly and thus to experience RI more readily with relatively higher intensity (Figs. 7a,e). In addition, the average RMW of TCs with RI (without RI) following RC tend to be smaller (larger) than 55 km (Figs. 7b,f), which is consistent with the findings by Wu and Ruan (2021), who revealed that TCs tend to experience RI often after the RMW contracts to a small size of ~55 km. Note that the results seem to be different from that in Fig. 4e, which shows that only large RMW cases (RMW  $\geq$  60 km) experience RC. This is because the RMW refers to the value at the current time exactly ( $t_0$ ) in Fig. 4 but at the time following the onset of RC ( $t_0$ + interval) in Fig. 7 as mentioned above.

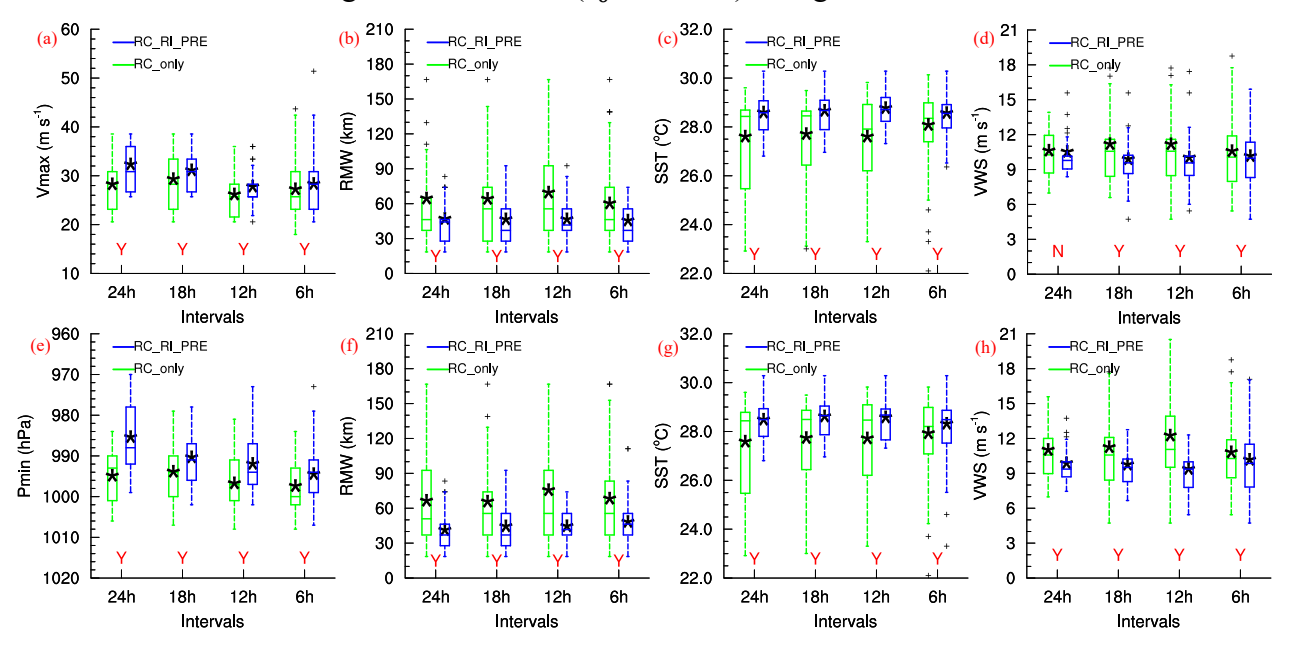


Figure 7. Boxplots of (a) TC intensity, (b) RMW, (c) sea surface temperature, and (d) vertical wind shear immediately following the onset time of RC for those TCs with RC preceding RI (RC\_RI\_PRE) and TCs with RC without RI (RC\_only) in the North Atlantic and Eastern North Pacific with the rate calculated using time intervals of 24 h, 18 h, 12 h, and 6 h. The letters "Y" and "N" indicate that the difference of the averaged values between RC\_RI\_PRE and RC\_only is and is not statistically significant at the 95% confidence level, respectively. (e)–(h) As in (a)–(d), but for TC intensity and RI are defined based on the central sea level pressure.

To address whether the occurrence of RI following an RC is affected by the large-scale environmental conditions, we used the interim reanalysis data from the European Centre for Medium-Range Weather Forecasts (ERA-Interim; Dee et al. 2011) and checked the differences in

sea surface temperature (SST) and vertical wind shear (VWS) between TCs with and without RI following an RC. The SST of each selected TC is defined as the average within a radius of 300 km from the TC center as in Fei et al. (2020). To obtain the environmental VWS, the disturbances in the original wind fields with wavelengths less than 1000 km are removed in both the zonal and meridional directions iteratively using the three-point smoothing operator of Kurihara et al. (1993), and then the VWS is calculated as the vector difference of horizontal winds averaged in the annulus between 200-800 km from the TC center between 200-850 hPa as in Fei et al. (2020). Consistent with previous statistical studies (e.g., Kaplan and DeMaria 2003; Xu and Wang 2015; Fudeyasu et al. 2018), TCs with RI following an RC tend to have more favorable environments, i.e., higher SST and lower VWS, than those without RI following an RC (Figs. 7c,d,g,h), with the differences being statistically significant at the 95% confidence level. This result is consistent for both the Vmaxbased and *Pmin*-based intensification rates and for all time intervals although the difference in the averaged VWS is not statistically significant for the 24-h time interval for the Vmax-based intensification rate (Fig. 7d). Note that the results do not mean that TCs with a high SST and low VWS would experience RI with RC, because some previous studies show no statistically significant differences in the environment conditions between TCs with and without RI (e.g., Hendricks et al. 2010). Since the statistical results could be potentially influenced by the study periods, basins, and statistical methods, future studies are needed to further examine the relationships between the environmental factors and the RI occurrence with and without RC.

Since the eyewall replacement cycle might potentially affect the occurrence of RI and RC (Mauk 2016), we have also checked the overall frequency distribution of TCs associated with RI or RC (as shown in Fig. 6) with those TCs likely experiencing eyewall replacement cycle before the lifetime maximum intensity removed. The information of eyewall replacement cycle is obtained from the product of Microwave-based Probability of Eyewall Replacement Cycle (M-PERC) model provided by the Space Science and Engineering Center at the University of Wisconsin-Madison (http://tropic.ssec.wisc.edu/real-time/archerOnline/web/ERC\_archive\_page.html). Because of the available M-PERC dataset only covers the period 1999–2011 for the North Atlantic, we only checked TCs in the North Atlantic during the period. We found that the overall frequency distributions with or without the eyewall replacement cycle TCs are qualitatively unchanged and are similar to those in Fig. 6 (not shown). With the eyewall replacement cycle TCs removed, the differences in intensity, RMW, and environmental conditions between TCs with and without RI

following an RC (i.e., Fig. 7) are also qualitatively unchanged (not shown). Considering the fact that the frequency of TCs with eyewall replacement cycles before the lifetime maximum intensity over the Eastern North Pacific is much less than that in the North Atlantic (Kossin and Sitkowski 2009; Mauk 2016), we can conclude that our main conclusions are not affected by the eyewall replacement cycle.

## 6. Preceding time

433

434

435

436

437

438

439

440

441

442

443

444

445

446

447

448

449

450

451

452

453

454

455

456

457

Although we have shown that the onset of RC tends to precede the onset of RI, we can also see that large variability exists in the preceding time (Figs. 5b.d). It is unclear what determines the preceding time of the onset of RC relative to the onset of RI. As a preliminary effort, we examined the relationship between the (non-negative) preceding time (with the outliers removed) and the TC intensity or RMW size immediately following the onset of RC with the results shown in Fig. 8. We can see that for both the *Vmax*-based and *Pmin*-based intensification rates and for all time intervals, the onset of RI tends to occur earlier after the onset of RC in TCs with larger TC intensity (Figs. 8a,e). The inverse correlation between the preceding time and TC intensity is statistically significant at the 95% confidence level under the student's t-test almost for all time intervals except for the 6-h interval for the *Pmin*-based intensification rate (Fig. 8e). The relationship between the preceding time and the RMW is similar for different time intervals and for both the Vmax-based and Pmin-based intensification rates (Figs. 8b,f). The onset of RI tends to lag further behind that of RC with larger RMW. The positive correlation is statistically significant at the 95% confidence level for the time intervals of 24 h, 18 h, and 12 h for the *Vmax*-based intensification rates (Fig. 8b) and for the time interval of 18 h for the Pmin-based intensification rate (Fig. 8f). As mentioned above, this is likely because a TC is easier to intensify rapidly with a relatively stronger intensity in the early intensification stage (Xu and Wang 2015; Li et al. 2021; Wang et al. 2021a,b) and after the RMW contracts to a certain small size (Xu and Wang 2015; Li et al. 2019; Wu and Ruan 2021; Li et al. 2021).

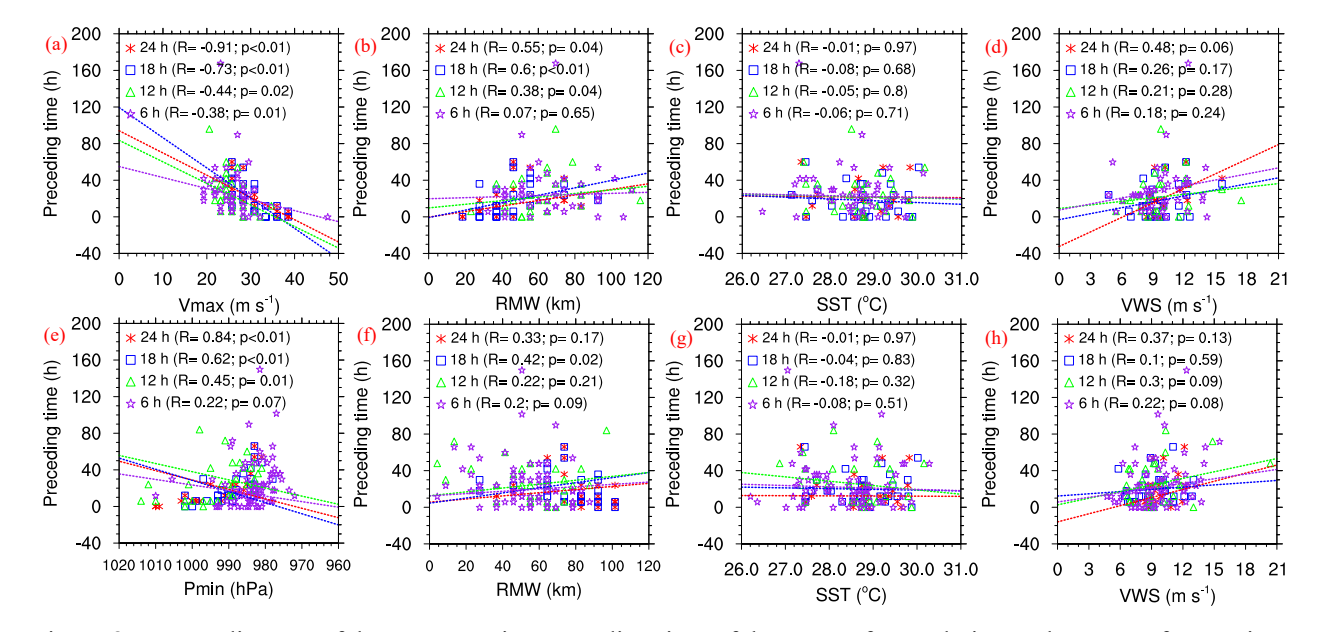


Figure 8. Scatter diagram of the non-negative preceding time of the onset of RC relative to the onset of RI against (a) TC intensity, (b) RMW, (c) sea surface temperature (SST), and (d) vertical wind shear (VWS) immediately following the onset time of RC for the time intervals of 24 h, 18 h, 12 h, and 6 h. For each time interval, the corresponding correlation coefficient (R) and the p-value under the student's t-test, with the outliers of preceding time removed, are shown in the parentheses following each legend. The corresponding regression line with the outliers removed for each time interval is also shown. (e)—(h) As in (a)—(d), but with TC intensity and RI being defined based on the central sea level pressure ( $P_{min}$ ).

458

459

460

461

462

463

464

465

466

467

468

469

470

471

472

473

474

475

476

477

478

479

480

481

To examine whether the preceding time is potentially affected by the large-scale environmental conditions, both the SST and VWS are evaluated as above, with the results shown in Figs. 8c,d,g,h. We can see that there is a general negative (positive) correlation between the preceding time and SST (VWS) for both the *Vmax*-based and *Pmin*-based intensification rates with different time intervals. This is as expected because higher SST or lower VWS often implies more favorable conditions for intensification and earlier RI onset (Li et al. 2021; Wang and Wu 2004), and also consistent with previous statistical studies (e.g., Kaplan and DeMaria 2003; Xu et al. 2016; Fudeyasu et al. 2018). Note that although the above results indicate the possible effects of SST and VWS on the preceding time of the onset of RC relative to the onset of RI, the correlations between the preceding time and SST and VWS are not statistically significant (Figs. 8c,g). This might be partly due to the small sample size (Fig. 5). We have also checked the temporal variations of SST and VWS during the period between the onset times of RC and RI and didn't find any obvious relationship between them with the preceding time (not shown). Our further check has also shown that the correlations between the preceding time and the averaged SST and VWS during the onset times of RC and RI are also not statistically significant (not shown).

Since there is a larger sample size in the comparison between the times of the peak RMW contraction rate and peak TC intensification rate (Fig. 1), it is our interest to examine the potential effect of those internal and environmental factors mentioned above on the preceding time of the peak RMW contraction rate relative to the peak intensification rate. Consistent with the patterns shown in Fig. 8, the preceding time of the peak RMW contraction rate relative to the peak intensification rate also tends to be shorter with higher TC intensity (Fig. 9a), smaller RMW (Fig. 9b), higher SST (Fig. 9c), and lower VWS (Fig. 9d). The relationships between the preceding time and TC intensity and RMW seem to be robust and are statistically significant at the 95% confidence level for all time intervals (Figs. 9a,b). The correlation between the preceding time and the environmental factors SST and VWS are less statistically significant for all time intervals, also similar to the preceding time of the onset of RC relative to the onset of RI (Figs. 8c,d,g,h). Based on the results of Figs. 8 and 9, we may conclude that the preceding time of the peak RMW contraction rate relative to the peak intensification rate and the onset of RC relative to the onset of RI in rapidly intensifying and contracting TCs are likely controlled by internal dynamical processes, which could be modified by environmental conditions to some extent.

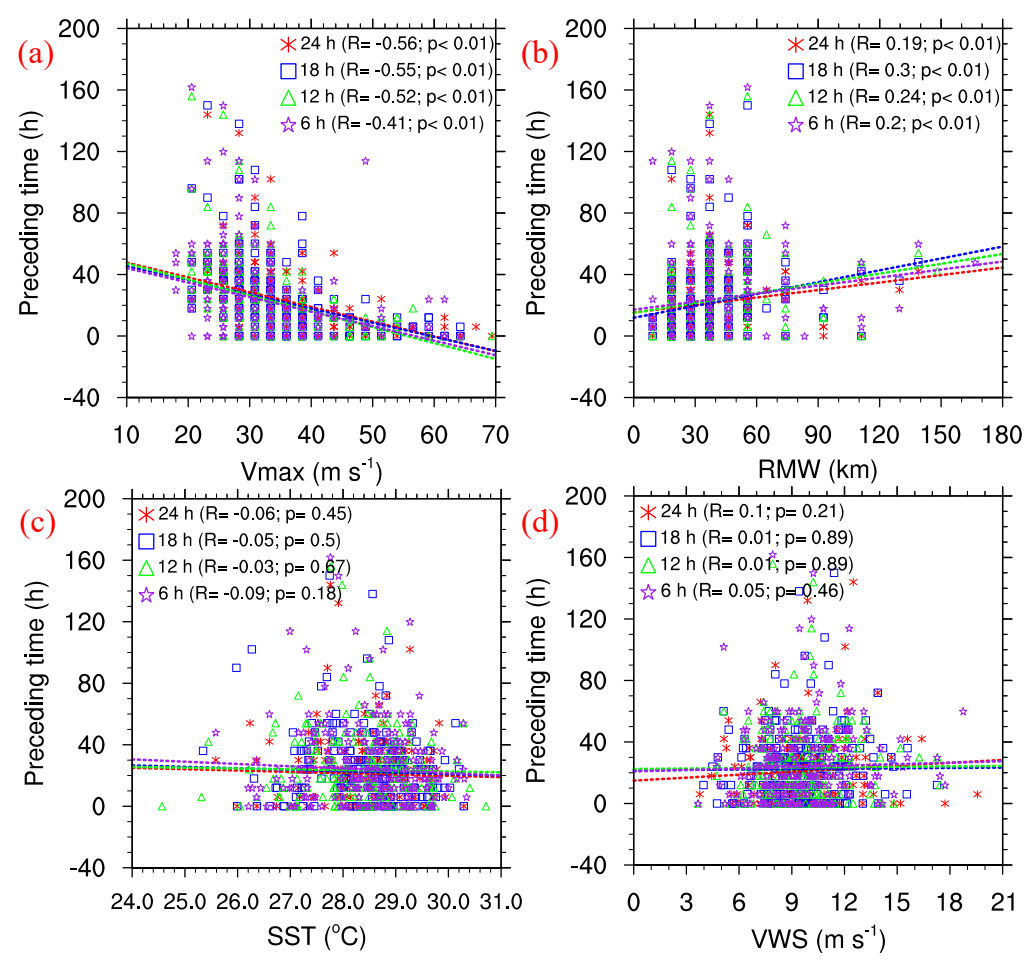


Figure 9. (a) Scatter diagram of the non-negative preceding time of the peak RMW contraction rate relative to the peak intensification rate against (a) TC intensity, (b) RMW, (c) sea surface temperature (SST), and (d) vertical wind shear (VWS) immediately following the time of peak RMW contraction rate with the time intervals of 24 h, 18 h, 12 h, and 6 h, respectively.

#### 7. Conclusions

In this study, the statistical relationship between RMW RC and TC RI is analyzed based on the EBT dataset for the North Atlantic and Eastern North Pacific during 1999–2019. Four different time intervals, viz., 24 h, 18 h, 12 h, and 6 h, are used to calculate the intensification/contraction rates for TCs that are tropical systems that are not affected by landmass and reach a lifetime maximum intensity at least 32 m s<sup>-1</sup>. Results show that for more than ~65% of the selected TCs, the time of the peak contraction rate precedes the time of the peak intensification rate, which is independent of the time interval used, with an average preceding time of ~10–15 h. Using the quantitatively defined RI and RC based on the EBT dataset, we find that the onset time of RC also predominantly precedes the onset time of RI in rapidly intensifying and contracting TCs, which is also independent of the time interval and the definition of RI. Our preliminary tests also indicate

that the main conclusions are not affected by the evewall replacement cycle. Overall, more than ~65% of the rapidly intensifying and contracting TCs involve the onset time of RC preceding the onset time of RI, on average, by ~15–25 h. The preceding time of the peak RMW contraction rate relative to the peak intensification rate, or that of the onset of RC relative to the onset of RI in rapidly intensifying and contracting TCs tends to be larger with weaker intensity or larger RMW size. In addition, a higher SST and lower VWS also favor a shorter preceding time. However, the relationships are mostly not statistically significant. The results suggest that the preceding time is probably controlled mainly by internal dynamical processes, which could be modified by environmental conditions to some extent. Note that we have excluded those records with the TC intensity below tropical storm when we compare the times of the peak RMW contraction rate and peak TC intensification rate (Fig. 1) or the onset times of RC and RI (Fig. 5). Although we have verified that the qualitative conclusions are not affected by this criterion, the quantitative conclusions are. Without this criterion, the ratios for the time of the peak contraction rate preceding the time of the peak intensification rate and for the onset time of RC preceding the onset time of RI increase slightly from more than ~65% to more than 70%, and the averaged differences in the time between the peak RMW contraction rate relative to the peak intensification rate and that of the onset of RC relative to the onset of RI increase from ~10-15 h and ~15-25 h to ~15-25 and ~25-40, respectively (not shown). This is understandable because more cases with large contraction rate occur during the weak intensity stage (cf. Fig. 4). However, considering the larger errors in measuring RMW for weaker TCs (cf. Kossin et al. 2007), we have not gone into details on the results during the weak intensity stage.

513

514

515

516

517

518

519

520

521

522

523

524

525

526

527

528

529

530

531

532

533

534

535

536

537

538

539

540

541

542

543

Results from this study demonstrate that rapid RMW contraction frequently precedes TC RI in rapidly intensifying and contracting TCs, consistent with the finding in Li et al. (2021). This is because as a TC intensifies in the early intensification stage, the TC intensity or inner-core diabatic heating often increases gradually and becomes favorable for increasing intensification rate, but the curvature of the radial profile of tangential wind also increases gradually and tend to reduce the increase in contraction rate (Stern et al. 2015; Li et al. 2021). However, results from this study and Li et al. (2021) do not mean that there must be an RI following an RC, as also indicated by Wu and Ruan (2021), due to deleterious environmental effects on TC intensification, such as oceanic cold core eddies and VWS. Our preliminary results have shown that ~50% TCs with RC experience RI, and TCs with stronger intensity, smaller RMW, and more favorable environmental conditions, such

as higher SST and lower VWS, tend to experience RI more readily following an RC. It will be a good topic for a future study to further understand the conditions for the occurrence of RI and RC and the dynamical processes and environmental factors that control the preceding time of the onset of RC relative to the onset of RI. These may provide a new perspective to help improve the prediction of the timing of RI based on the onset time of RC.

Another remaining and interesting issue is the overall higher intensification rate in the Eastern North Pacific than in the North Atlantic, but the higher contraction rate in the North Atlantic than in the Eastern North Pacific, in particular, for the time intervals of 24 h and 18 h (Table 1). This may suggest that the intensification rate is not necessarily associated with the contraction rate. Our preliminary test also indicates that there is no significant correlation between the peak intensification rate and peak contraction rate in both basins (not shown). A detailed analysis is beyond the scope of this study, but it will be a good topic for a future study to understand the possible relationship between the intensification rate and the contraction rate from theory, numerical simulations, and observational analysis. Another topic for a future study is to further understand the conditions for the occurrence of RI and RC and the dynamical processes and environmental factors that control the preceding time of the onset of RC relative to the onset of RI.

560 Acknowledgments.

544

545

546

547

548

549

550

551

552

553

554

555

556

557

558

559

- The authors would be grateful to Dr. Rachel Mauk and two anonymous reviewers for their
- constructive and critical review comments. Y. Li thanks Dr. Qiaoyan Wu for helpful discussions
- in the early stage of this work. This study was supported in part by National Natural Science
- Foundation of China under grants 41730960 and 42192555 and the National Key R&D Program
- of China under grant 2017YFC1501602 and in part by NSF grant AGS-1834300. Y. Li is also
- supported partly by China Postdoctoral Science Foundation (BX2021121; 2021M700066).
- 567 Data Availability Statement.
- 568 The EBT data were obtained from https://rammb2.cira.colostate.edu/research/tropical-
- 569 cyclones/tc extended best track dataset/. The ERA-Interim data were obtained from
- 570 https://apps.ecmwf.int/datasets/.

571 REFERENCES

- 572 Chen, H., D. Zhang, J. Carton, and R. Atlas, 2011: On the rapid intensification of Hurricane Wilma
- 573 (2005). Part I: Model prediction and structural changes. Wea. Forecasting, 26, 885–
- 574 901, https://doi.org/10.1175/WAF-D-11-00001.1.
- 575 Corbosiero, K. L., J. Molinari, and M. L. Black, 2005: The structure and evolution of Hurricane
- Elena (1985). Part I: Symmetric intensification, Mon. Wea. Rev., 133, 2905–2921,
- 577 https://doi.org/10.1175/MWR3010.1.
- Dee, D. P., and Coauthors, 2011: The ERA-Interim reanalysis: Configuration and performance of
- the data assimilation system. Quart. J. Roy. Meteor. Soc., 137, 553-597, https://doi.org/
- 580 10.1002/qj.828.
- Demuth, J. L., M. DeMaria, J. A. Knaff, and T. H. Vonder Haar, 2004: Evaluation of advanced
- microwave sounding unit tropical-cyclone intensity and size estimation algorithms. J. Appl.
- 583 *Meteor. Climatol.*, 43, 282–296, https://doi.org/10.1175/1520-0450(2004)043%3C0282:
- 584 EOAMSU%3E2.0.CO;2.
- Demuth, J., M. DeMaria, and J. A. Knaff, 2006: Improvement of Advanced Microwave Sounder
- Unit tropical cyclone intensity and size estimation algorithms. J. Appl. Meteor. Climatol., 45,
- 587 1573–1581, https://doi.org/10.1175/JAM2429.1.
- Emanuel, K., 1997: Some aspects of hurricane inner-core dynamics and energetics. J. Atmos. Sci.,
- 54, 1014–1026, https://doi.org/10.1175/1520-0469(1997)054,1014:SAOHIC.2.0.CO;2.
- Emanuel, K., 2018: 100 years of progress in tropical cyclone research. A Century of Progress in
- 591 Atmospheric and Related Sciences: Celebrating the American Meteorological Society
- 592 Centennial, Meteor. Monogr., No. 59, Amer. Meteor. Soc.,
- 593 https://doi.org/10.1175/AMSMONOGRAPHS-D-18-0016.1.
- 594 Fei, R., J. Xu, Y. Wang, and C. Yang, 2020: Factors affecting the weakening rate of tropical
- 595 cyclones over the western North Pacific. Mon. Wea. Rev., 148, 3693–3712,
- 596 https://doi.org/10.1175/MWR-D-19-0356.1.
- 597 Fudeyasu, H., K. Ito, and Y. Miyamoto, 2018: Characteristics of tropical cyclone rapid
- intensification over the Western North Pacific. J. Climate, 31, 8917–8930.
- 599 https://doi.org/10.1175/JCLI-D-17-0653.1.
- Kaplan, J., and M. DeMaria, 2003: Large-scale characteristics of rapidly intensifying tropical
- 601 cyclones in the North Atlantic basin. Wea. Forecasting, 18, 1093–1108,

- 602 https://doi.org/10.1175/1520-0434(2003)018,1093: LCORIT.2.0.CO;2.
- Kaplan, J., M. DeMaria, and J. A. Knaff, 2010: A revised tropical cyclone rapid intensification
- index for the Atlantic and Eastern North Pacific basins. Wea. Forecasting, 25, 220–241,
- 605 https://doi.org/10.1175/2009WAF2222280.1.
- Kaplan, J., C. M. Rozoff, M. DeMaria, C. R. Sampson, J. P. Sampson, C. S. Velden, J. J. Cione, J.
- P. Dunion, J. A. Knaff, J. A. Zhang, J. F. Dostalek, J. D. Hawkins, T. F. Lee, and J. E. Solbrig,
- 608 2015: Evaluating environmental impacts on tropical cyclone rapid intensification
- predictability utilizing statistical models. Wea. Forecasting, 30, 1374–1396,
- 610 https://doi.org/10.1175/WAF-D-15-0032.1.
- Kantha, L., 2006: Time to replace the Saffir–Simpson hurricane scale? *Eos, Trans. Amer. Geophys.*
- *Union*, **87**, 3–6, https://doi.org/10.1029/2006EO010003.
- Kimball, S. K., and M. S. Mulekar, 2004: A 15-year climatology of North Atlantic tropical cyclones.
- Part I: Size parameters. *J. Climate*, 17, 3555–3575, https://doi.org/10.1175/1520-
- 615 0442(2004)017%3C3555:AYCONA%3E2.0.CO;2.
- Klotzbach, P. J., Bell, M. M., Bowen, S. G., Gibney, E. J., Knapp, K. R., and Schreck III, C. J.,
- 617 2020: Surface Pressure a more Skillful Predictor of normalized hurricane damage than
- Maximum Sustained wind. Bull. Amer. Meteor. Soc., 101, E830–E846.
- 619 https://doi.org/10.1175/BAMS-D-19-0062.1.
- Knaff, J. A., C. R. Sampson, B. R. Strahl, 2020: A tropical cyclone rapid intensification prediction
- aid for the Joint Typhoon Warning Center's areas of responsibility. Wea. Forecasting, 35,
- 622 1173–1185, https://doi.org/10.1175/WAF-D-19-0228.1.
- Kossin J P., and M. Sitkowski, 2009: An objective model for identifying secondary eyewall
- formation in hurricanes. Mon. Wea. Rev., 137, 876–892,
- https://doi.org/10.1175/2008MWR2701.1.
- Kossin, J. P., J. A. Knaff, H. I. Berger, D. C. Herndon, T. A. Cram, C. S. Velden, R. J. Murnane,
- and J. D. Hawkins, 2007: Estimating hurricane wind structure in the absence of aircraft
- 628 reconnaissance, *Wea. Forecasting*, **22**, 89–101, https://doi.org/10.1175/WAF985.1.
- 629 Kurihara, Y., M. A. Bender, and R. J. Ross, 1993: An initialization scheme of hurricane models
- by vortex specification. *Mon. Wea. Rev.*, **121**, 2030–2045, https://doi.org/10.1175/1520-
- 631 0493(1993)121<2030:AISOHM>2.0.CO;2.
- Landsea, C. W., and J. L. Franklin, 2013: Atlantic hurricane database uncertainty and presentation

- of a new database format. Mon. Wea. Rev., 141, 3576–3592, https://doi.org/10.1175/MWR-
- 634 D-12-00254.1.
- 635 Li, Y., Y. Wang, and Y. Lin, 2019: Revisiting the dynamics of eyewall contraction of tropical
- 636 cyclones. J. Atmos. Sci., **76**, 3229–3245, https://doi.org/10.1175/JAS-D-19-0076.1.
- 637 Li, Y., Y. Wang, and Y. Lin, 2020: How much does the upward advection of the supergradient
- component of boundary layer wind contribute to tropical cyclone intensification and
- 639 maximum intensity? J. Atmos. Sci., 77, 2649–2664, https://doi.org/10.1175/JAS-D-19-0350.1.
- 640 Li, Y., Y. Wang, Y. Lin, and X. Wang, 2021: Why does rapid contraction of the radius of maximum
- wind precede rapid intensification in tropical cyclones? J. Atmos. Sci., 78, 3441–3453,
- 642 https://doi.org/10.1175/JAS-D-21-0129.1.
- Mainelli, M., M. DeMaria, L. K. Shay, and G. Goni, 2008: Application of oceanic heat content
- estimation to operational forecasting of recent Atlantic category 5 hurricanes, Wea.
- *Forecasting*, **23**, 3-16, https://doi.org/10.1175/2007WAF2006111.1.
- Mauk R. G., 2016: Prediction of intensity change subsequent to concentric eyewall events. Ph.D.
- Ohio State University, 306 pp. http://rave.ohiolink.edu/etdc/view?acc\_num=osu1469037273.
- Qin, N., D.-L. Zhang, and Y. Li, 2016: A statistical analysis of steady eyewall sizes associated with
- rapidly intensifying hurricanes. Wea. Forecasting, 31, 737–742, https://doi.org/10.1175/
- 650 WAF-D-16-0016.1.
- 651 Schubert, W. H., and J. J. Hack, 1982: Inertial stability and tropical cyclone development. *J. Atmos.*
- 652 Sci., **39**, 1687–1697, https://doi.org/10.1175/1520-0469(1982)039,1687:ISATCD.2.0.CO;2.
- Shapiro, L. J., and H. E. Willoughby, 1982: The response of balanced hurricanes to local sources
- of heat and momentum. *J. Atmos. Sci.*, **39**, 378–394, https://doi.org/10.1175/1520-0469(1982)
- 655 039.0378:TROBHT.2.0.CO;2.
- 656 Shimada, U., and T. Horinouchi, 2018: Reintensification and eyewall formation in strong shear: A
- 657 case study of Typhoon Noul (2015). *Mon. Wea. Rev.*, **146**, 2799–2817,
- https://doi.org/10.1175/MWR-D-18-0035.1.
- 659 Stern, D. P., J. L. Vigh, D. S. Nolan, and F. Zhang, 2015: Revisiting the relationship between
- eyewall contraction and intensification. J. Atmos. Sci., 72, 1283–1306, https://doi.org/
- 661 10.1175/JAS-D-14-0261.1.

- Willoughby, H. E., 1990: Temporal changes of the primary circulation in tropical cyclones. J.
- 663 Atmos. Sci., 47, 242–264, https://doi.org/10.1175/1520-0469(1990)047,0242:TCOTPC.
- 664 2.0.CO;2.
- Wang, Y., and C.-C. Wu, 2004: Current understanding of tropical cyclone structure and intensity
- changes a review, *Meteorol. Atmos. Phys.*, **87**, 257–278. https://doi.org/10.1007/s00703-
- 667 003-0055-6.
- Wang, Y., Y. Li, and J. Xu, 2021a: A new time-dependent theory of tropical cyclone intensification.
- *J. Atmos. Sci.*, **78**, 3855–3865, https://doi.org/10.1175/JAS-D-21-0169.1.
- Wang, Y., Y. Li, J. Xu, Z.-M. Tan, and Y. Lin, 2021b: The intensity dependence of tropical cyclone
- intensification rate in a simplified energetically based dynamical system model. *J. Atmos. Sci.*,
- **78**, 2033–2045, https://doi.org/10.1175/JAS-D-20-0393.1.
- Willoughby, H. E., J. A. Clos, and M. G. Shoreibah, 1982: Concentric eye walls, secondary wind
- maxima, and the evolution of the hurricane vortex. J. Atmos. Sci., 39, 395-411,
- 675 https://doi.org/10.1175/1520-0469(1982)039,0395:CEWSWM.2.0.CO;2.
- Wu, Q., and Z. Ruan, 2021: Rapid contraction of the radius of maximum tangential wind and rapid
- intensification of a tropical cyclone. J. Geophys. Res. Atmos., 126, e2020JD033681,
- 678 https://doi.org/10.1029/2020JD033681.
- 679 Xu, J., and Y. Wang, 2015: A statistical analysis on the development of tropical cyclone
- intensification rate on the storm intensity and size in the North Atlantic. Wea. Forecasting,
- **30**, 692–701, https://doi.org/10.1175/WAF-D-14-00141.1.
- Ku, J., Y. Wang, and Z.-M. Tan, 2016; The relationship between sea surface temperature and
- maximum intensification rate of tropical cyclones in the North Atlantic. Wea. Forecasting, 73,
- 4979–4988, https://doi.org/10.1175/JAS-D-16-0164.1.